Colloid Polym Sci (2008) 286:1605–1612
DOI 10.1007/s00396-008-1934-7

ORIGINAL CONTRIBUTION

Preparation and characterization of poly(styrene-alt-maleic acid)-*b*-polystyrene block copolymer self-assembled nanoparticles

Jingtian Han · Patrick Silcock · A. James McQuillan · Phil Bremer

Received: 29 July 2007 / Revised: 8 September 2008 / Accepted: 17 September 2008 / Published online: 16 October 2008

Abstract Block copolymers poly(styrene-alt-maleic anhydride)-*b*-polystyrene (P(St-alt-MAn)-*b*-PSt) were synthesized via radical addition fragmentation chain transfer copolymerization. The maleic anhydride-containing segments of the block copolymer were hydrolyzed to form amphiphilic poly (styrene-alt-maleic acid)-*b*-polystyrene (P(St-alt-MA)-*b*-PSt). In aqueous solution, P(St-alt-MA)$_{73}$-*b*-PSt$_{81}$ and P(St-alt-MA)$_{58}$-*b*-PSt$_{130}$ formed stable dispersed spherical aggregates of approximately 25 and 40 nm, respectively. Particle size was stable under alkaline conditions and was little affected by the polymer concentration in the range of 0.025–1.0 mg mL^{-1}. The critical aggregation concentrations of the block copolymer self-aggregates were 1×10^{-3} and 3×10^{-3} mg mL^{-1} for hydrophobic PSt block lengths of 130 and 81 monomer units, respectively. The nanoparticles had a negative surface charge at pH>2. Scanning electron microscopy images revealed that particle–particle coalescence did not occur upon drying of the film and the nanoparticles remained discrete. Controlled aspirin release from the nanoparticles was dependent on the structure of the block polymers and release medium.

Keywords Polymer nanoparticles · Self-aggregation · Diblock copolymer · RAFT copolymerization · Controlled release

Electronic supplementary material The online version of this article (doi:10.1007/s00396-008-1934-7) contains supplementary material, which is available to authorized users.

J. Han · P. Silcock (✉) · P. Bremer
Department of Food Science, University of Otago,
P.O. Box 56, Dunedin, New Zealand
e-mail: pat.silcock@stonebow.otago.ac.nz

A. J. McQuillan
Department of Chemistry, University of Otago,
P.O. Box 56, Dunedin, New Zealand

Introduction

Micelle-like aggregates formed with amphiphilic diblock copolymers are of interest due to their potential biotechnological and pharmaceutical applications [1, 2]. These nanosized micelle-like aggregates of various morphologies form in aqueous solution due to the limited water solubility of the hydrophobic block and the hydrophobic interactions between the water-insoluble segments on exposure to aqueous environments. Polymeric micelles in aqueous media are characterized by small size (approximately 10–100 nm), a hydrophobic core, and a hydrophilic corona or outer shell that plays a role in controlling reactions between the core and the external environment. These amphiphilic "nanocarrier" particles are of interest as they are capable of solubilizing, protecting, and releasing a wide variety of active compounds, such as lipophilic drugs or antimicrobial agents into diverse environments ranging from the human body to cosmetic systems and aquatic environments [3, 4]. Furthermore, these nanosized aggregates posses the advantages of: a fairly narrow size distribution; a low critical aggregation concentration (CAC), ensuring their stability after dilution [3]; a slow rate of dissociation and thereby a slow release of the active; and have a high drug loading capacity. Amphiphilic block copolymers reported to date have had either polystyrene, poly(caprolactone), or poly (lactic acid) as the hydrophobic segment and poly(ethylene glycol), poly(acrylic acid), or poly(isopropylacrylamide) as the hydrophilic segment [5–8].

In this study, we report on the self-aggregation behavior of a block copolymer which has polystyrene as the hydrophobic segment and poly(styrene-alt-maleic acid) as the hydrophilic outer shell. These stable self-assembled nanoparticles were formed by a precipitation and dialysis method and were characterized with dynamic laser light

scattering (DLLS), fluorescence spectroscopy, transmission electron microscope (TEM), and scanning electron microscope (SEM). The composition of soluble segments present in the outer shell resulted in nanoparticles which differed in their charge distribution and functional properties from other negatively charged nanoparticles produced using polyacrylic acid (PAA) [9]. The drug loading and releasing profile of aspirin in the nanoparticles was evaluated. The stability of the drug-loaded nanoparticles and the release profiles of aspirin were evaluated. We are currently carrying out further studies using nanoparticle films to determine their response to variations in external pH, external ionic strength, and the rate of protein adhesion.

Experimental section

Materials

Styrene (99%) was purchased from Merck (Schuchardt OHG, Germany) and purified by distillation under vacuum before use. Maleic anhydride (99%, Acros, USA) was recrystallized from anhydrous chloroform free of ethanol. Azobis(isobutyronitrile) (AIBN, 98%) was obtained from Acros (USA) and recrystallized in methanol. Phosphorus pentasulfide (99%, Aldrich), benzyl alcohol (99%), and benzoic acid (99.9%, BDH Chemicals) were used as received. Aspirin (>99%) was supplied by Sigma Aldrich. All other solvents were analytical or high-performance liquid chromatography (HPLC) grade. Water used was Milli-Q (Millipore).

Preparation of P(St-alt-MAn)-*b*-PSt via RAFT polymerization

The block copolymers were synthesized by a previously reported method [10–12] with slight modifications using the dithioester chain transfer agent (*S*)-benzyl dithiobenzoate (BTBA), which was synthesized according to a procedure described by Sudalai [13]. The polymers were characterized by gel permeation chromatography, elemental analysis, nuclear magnetic resonance (NMR), and differential scanning calorimetry.

Preparation of P(St-alt-MA)-*b*-PSt amphiphilic diblock copolymer

P(St-alt-MAn)-*b*-PSt solution in dimethylformamide (DMF) (10 mL, 0.2 g mL^{-1}) was added dropwise into a NaOH aqueous solution (50 mL, 20 wt.%) at 70 °C and held at this temperature overnight [5, 7, 11]. The hydrolysate of the block copolymer was precipitated by adding the solution dropwise into hydrochloric acid (40 mL, 33 vol.%). The precipitate was centrifuged and washed successively with dilute hydrochloric acid (5 vol.%) and water, each for six times. The product was dried at 50 °C in a vacuum oven for 24 h.

Amphiphilic block copolymer nanoparticles self-assembly

Self-assembly of the polymeric nanoparticles was achieved by the addition of P(St-alt-MA)$_m$-*b*-PSt$_n$ copolymer solution in DMF (2.0 mL, 10 mg mL^{-1}) into 20 mL of water at the rate of one drop (about 0.01 mL) every 10 s using a microsyringe. The nanoparticle suspension was stirred during addition and for a further 24 h, then dialyzed against water for 7 days. Prior to the particle size measurements, the polymer suspensions (0.1 mg mL^{-1}) were sonicated for 2 min and passed through a 0.45-μm filter (Millipore).

ATR-IR spectroscopy

Infrared (IR) spectra were recorded using a DigiLab FTS 4000 spectrometer. A ZnSe single-reflection attenuated total reflectance (ATR) prism was cleaned by polishing with 0.015 μm Al_2O_3 powder, washed with water, and dried under vacuum. A 200-μL volume of the polymer solution in tetrahydrofuran (THF; 2.0 mg mL^{-1}) was deposited onto the ZnSe prism. After removing the solvent under reduced pressure, the polymer IR spectra were constructed using the Merlin 3.4 software from 64 scans at 4 cm^{-1} resolution.

Measurement of dynamic light scattering

The size distribution of the nanoparticles was measured at 25 °C using a DLLS instrument (HPP5001 Malvern Instruments, UK) equipped with a He–Ne laser with a scattering angle of 90°. The particle size and size distribution were calculated using nonnegative least squares algorithms [4, 14].

Fluorescence spectroscopy of pyrene-containing nanoparticles

The self-aggregation behavior and CACs of the amphiphilic diblock copolymers in aqueous media were investigated as described by Choi [6] using pyrene as a fluorescence probe [4, 15, 16]. Pyrene fluorescence spectra were obtained using a spectrofluorophotometer (LS50B Fluorimeter, Perkin Elmer) with an excitation wavelength of 340 nm.

Zeta-potential measurements and the Debye plot

The zeta-potentials and the Debye plot of the self-assembled polymeric nanoparticles were determined using

a Zetasizer Nano ZS (Malvern Instruments, UK) at 25 °C. The pH of the nanoparticle suspensions (0.1 mg mL^{-1}) was adjusted with either NaOH or HCl solutions. The Debye plots were obtained using static light scattering (SLS) in the polymer concentration ranges from 0.2 to 0.5 mg/mL at pH 6.95 and 2.50. The measurements of the differential refractive index increment d*n*/d*c* of the nanoparticle suspensions were made with an Abbe refractometer.

Scanning electron microscopy

The surface morphology of the block polymer nanoparticles film was examined using a JEOL 6700F Field Emission SEM (JEOL, Japan). A 200-μL sample of the nanoparticle suspension (0.5 mg mL^{-1}, $D \approx 25$ nm) was deposited onto a glass slide and dried under vacuum at room temperature. The estimated thickness of the polymer nanoparticle film was around 1.0 μm. Samples were sputter coated with approximately 5 nm of Cr in an Emitech K250 coating attachment (Emitech, UK). Samples were viewed and imaged at 3 kV using a LEI detector.

Transmission electron microscopy

The morphology of the nanoparticles was observed using a TEM according to the method described by Joeng [4]. A drop of nanoparticle suspension containing 0.1% phosphotungstic acid (PTA) was placed onto a copper grid coated with carbon film. The grid was held horizontally for 30 s to allow the aggregates to settle and then vertically to allow excess fluid to drain. Imaging was carried out at 80 kV with a Philips EM CM100 TEM.

Loading and release of aspirin

Aspirin (10 mg) and polymer (10 mg) were dissolved in 2.0 mL of DMF. The solution was dialyzed against 1,000 mL of distilled water for 24 h. The amount of aspirin associated with the polymer (loaded) was determined by UV absorption of lyophilized aspirin-loaded polymer solution in DMF at 282 nm and confirmed by measuring the aspirin concentration in the dialysis media at 272 nm.

After dialysis, the dialysis tubes containing aspirin-loaded nanoparticles suspension were directly immersed into 100 mL of either distilled water (pH 6.14) or phosphate buffer (pH 7.43), respectively. At regular time intervals, 1.0 mL samples were taken from the release medium. The volume of the solution was held constant by the addition 1.0 mL of fresh solution. The amount of released aspirin was determined by measuring the absorbance at 272 nm. The release experiments were performed in duplicate.

Results and discussion

Synthesis and characterization of P(St-alt-MAn)-*b*-PSt and amphiphilic P(St-alt-MA)-*b*-PSt block copolymer

Using an initial molar ratio of styrene to maleic anhydride of either 9:1 (polymer 1) or 209:41 (polymer 2), two block copolymers were prepared from styrene and maleic anhydride via radical addition fragmentation chain transfer (RAFT) copolymerization with the generic formula of P(St-alt-MAn)$_m$-*b*-PSt$_n$. A copolymer (polymer 3) with the monomer feed 1:1 (St/MAn) of molar ratio was also prepared as a reference sample under the same polymerization conditions. The copolymers molecular weights (M_w, M_n) and their polydispersity index (PDI) were determined by gel permeation chromatography (GPC) (Table 1).

Based on the molecular weight measurements and the elemental analysis results (Table 2), the structures of the styrene- and maleic anhydride-based block copolymers were calculated as P(St-alt-MAn)$_{58}$-*b*-PSt$_{130}$ and P(St-alt-MAn)$_{73}$-*b*-PSt$_{81}$.The composition of the polymers were confirmed by ^{1}H NMR analysis [12]. The infrared spectra of P(St-alt-MAn)$_{58}$-*b*-PSt$_{130}$ showed the presence of anhydride peaks at 1,776 and 1,854 cm^{-1} (Fig. 1a).

The block copolymers displayed two distinct glass transition temperatures (T_g) of 92 and 174 °C for P(St-alt-MAn)$_{58}$-*b*-PSt$_{130}$ and at 80 and 175 °C for P(St-alt-MAn)$_{73}$-*b*-PSt$_{81}$ corresponding to the PSt and P(St-alt-MAn) block regions, respectively. Polymer 3, obtained from the reaction mixture with a monomers feed ratio of 1:1 after 4 h polymerization, had only one T_g at 176 °C, which was very close to the T_g of the P(St-alt-MAn) segment present in the block copolymers. This data strongly supports the conclusion that the final product is a block copolymer [10, 11, 17].

Table 1 Molecular weight, molecular weight distribution, and composition of block copolymers obtained via RAFT polymerization

Copolymer	Formula	M_w	M_n	PDI	Styrene in copolymer (mol%)
Polymer-1	P(St-alt-MAn)$_{58}$-*b*-PSt$_{130}$	33,500	25,300	1.33	76.42
Polymer-2	P(St-alt-MAn)$_{73}$-*b*-PSt$_{81}$	30,700	23,300	1.32	67.84
Polymer-3	P(St-alt-MAn)$_{103}$	26,700	20,900	1.27	49.12

M_w was determined from the polystyrene standard curve
M_n and M_w the number and weight molecular weight averages, respectively, *PDI* polydispersity index (PDI=M_w/M_n)

Table 2 Elemental analysis of the block copolymers based on maleic anhydride and styrene

Elements	$P(St\text{-}alt\text{-}MAn)_{58}$-*b*-$PSt_{130}$		$P(St\text{-}alt\text{-}MAn)_{73}$-*b*-$PSt_{81}$	
	Measured (%)	Calculated (%)	Measured (%)	Calculated (%)
C	82.46±0.02	82.55	78.68±0.08	78.73
H	6.46±0.06	6.42	6.21±0.13	5.95
O	11.09±0.08	11.03	15.11±0.05	15.12

The copolymerization of St with MAn copolymers exhibited some interesting features. MAn itself does not homopolymerize and its copolymerization with St has a strong tendency toward alternation [18]. It would normally be expected that under free radical polymerization conditions, a homopolystyrene and various styrene/maleic anhydride copolymers with a wide range of molecular weights and a large PDI would be produced [11, 17, 19]. However, by employing AIBN as the initiator and BTBA as a chain transfer regent at 60 °C in dioxane, a living free radical polymerization made it possible to produce a well-defined diblock copolymer with a narrow molecular weight distribution. This result suggests that the chain transfer agent in RAFT polymerization is necessary for the preparation of well-structured block copolymers based on styrene and maleic anhydride. Zhu and coworkers reported [11] that, under the same conditions, the absolute molar conversion of MAn and styrene was approximately equal until 80% of total MAn was consumed, suggesting that the copolymer will posses a predominantly alternating character until MAn is exhausted. Benoit et al. [17] also confirmed that the rate of polymerization of a 9:1 mixture of styrene and maleic anhydride was dramatically higher than for pure styrene with >90% conversion being obtained after 1 h at 120 °C when 2,2,6,6-tetramethylpiperidinyloxy was used as a chain transfer agent. In both systems, the reaction involved polymerization of styrene and maleic anhydride in a 1:1 molar ratio. After MAn was completely consumed, the alternating copolymer chain formed another block composed solely of PSt segment resulting in the formation of diblock copolymer with an initially P(St-alt-MAn) segment and PSt tail. The PDIs of the block copolymers produced in the current work were in the range of 1.2–1.3, which is in agreement with previously reported values for this polymer [20, 21].

The IR spectrum of the hydrolyzed amphiphilic block copolymer of $P(St\text{-}alt\text{-}MA)_{58}$-*b*-$PSt_{130}$ (Fig. 1b) shows that the anhydride peaks at 1,776 and 1,854 cm^{-1} that were present in the unhydrolyzed polymer have been replaced by a characteristic absorption for carboxylic acid at 1,725 cm^{-1}, indicating the hydrolysis of $P(St\text{-}alt\text{-}MAn)_{58}$-*b*-$PSt_{130}$.

Preparation and properties of self-assembled nanoparticles

The amphiphilic block copolymer with hydrophilic P(St-alt-MA) and hydrophobic PSt block segments formed micelle-like aggregates in an aqueous environment. In the aggregates, the PSt block aggregated to form a hydrophobic domain (core) and remained in an amorphous state at room temperature. The soluble segments P(St-alt-MA) acted as an exterior hydrophilic corona (or shell). The transmission electron micrograph of $P(St\text{-}alt\text{-}MA)_{73}$-*b*-$PSt_{81}$ with 0.1% PTA negative staining (Fig. 2) clearly shows uniform spherical nanoparticles with diameters of approximately 25 nm as a light zone surrounded by the dark negative stain [4]. This structure is in agreement with previously postulated structures for similar aggregated polymer nanoparticles [6, 7, 22].

The Debye plots of the polymer nanoparticle suspensions were obtained using SLS at pH 6.95. Based on the differential refractive index increment d*n*/d*c* (0.173 mLg^{-1}) measured with an Abbe refractometer, the weight-average molar masses were 6.104×10^6 and 3.180×10^6 $gmol^{-1}$ and the apparent aggregation numbers N^{agg} calculated to be 241 and 136 for $P(St\text{-}alt\text{-}MA)_{58}$-*b*-$PSt_{130}$ and $P(St\text{-}alt\text{-}MA)_{73}$-*b*-$PSt_{81}$ nanoparticles, respectively.

The aggregation behavior of the amphiphilic diblock copolymers in aqueous media was investigated using pyrene as a fluorescence probe. In a polar environment, pyrene has weak fluorescence intensity but when it is incorporated into a nonpolar particle core it strongly fluoresces. This change in the intensity of the fluorescence has previously been used to calculate the CAC of amphiphilic block copolymers in an aqueous phase [6, 20, 23–25]. The impact of varying the $P(St\text{-}alt\text{-}MA)_m$-*b*-$PSt_n$ concentration on the fluorescence emission spectra is

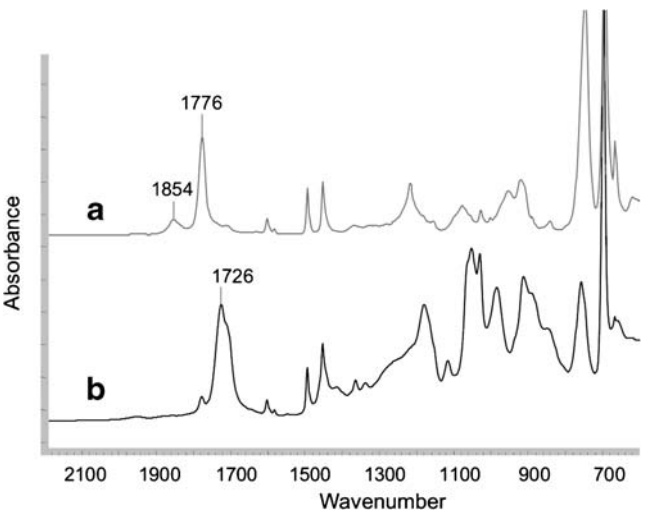

Fig. 1 ATR-IR spectra of **a** $P(St\text{-}alt\text{-}MAn)_{58}$-*b*-$PSt_{130}$ and **b** the hydrolyzed amphiphilic polymer $P(St\text{-}alt\text{-}MA)_{58}$-*b*-$PSt_{130}$

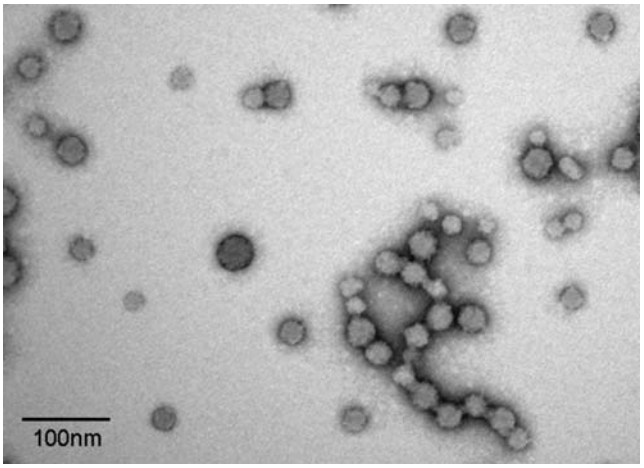

Fig. 2 TEM of P(St-alt-MA)$_{73}$-*b*-PSt$_{81}$ nanoparticles with 0.1% PTA negative staining

shown in Fig. 3. At low concentrations (c<CAC), there were negligible changes in total fluorescence emission intensity at 373 nm. Above the CAC, however, it increased sharply (Fig. 4). Based on the intensity versus concentration data, the CAC values of P(St-alt-MA)$_m$-*b*-PSt$_n$ were calculated to be 1.0×10^{-3} (m=58, n=130) and 2.99×10^{-3} mg mL^{-1} (m=73, n=81). These CAC concentrations are lower than those reported for a polyethylene glycol (PEO)-grafted block copolymer, which was in the range of 0.01–0.23 mg mL^{-1} [20]. This difference may be due to the shorter hydrophilic chain of the P(St-alt-MA)$_m$-*b*-PSt$_n$ amphiphilic diblock copolymer which decreases its solubility in aqueous media compared to the PEO-grafted block copolymer.

Particle size measurements using DLLS showed that the aggregated polymers formed monodispersed nanoparticles with a size distribution in the range of 20–30 nm (average

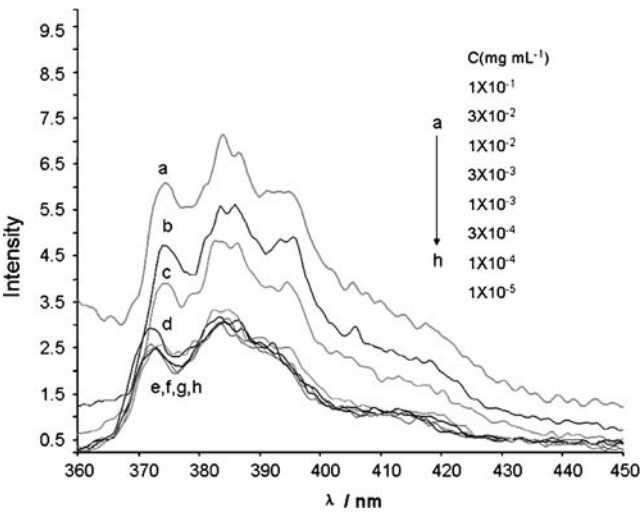

Fig. 3 Emission spectra of pyrene (6.0×10^{-7} mol L^{-1}) in the presence of P(St-alt-MAn)$_{58}$-*b*-PSt$_{130}$ at various concentrations (excitation wavelength was 340 nm)

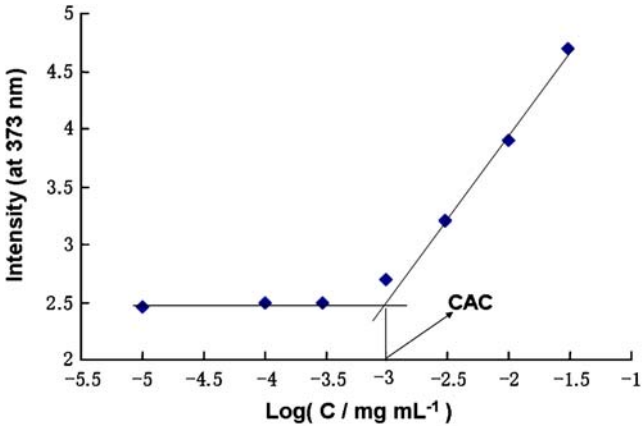

Fig. 4 Fluorescence intensity (at 373 nm) of pyrene versus the logarithm of P(St-alt-MAn)$_{58}$-*b*-PSt$_{130}$ concentration

approximately 25 nm) and 35–45 nm (average approximately 40 nm) for P(St-alt-MA)$_{73}$-*b*-PSt$_{81}$ and P(St-alt-MA)$_{58}$-*b*-PSt$_{130}$, respectively (Fig. 5). It has been reported that at a low ionic strength and a pH above 5, PAA chains are stretched to nearly their full length [26] with an effective length (not bond length) of 0.25 nm per repeating unit [27]. If the outer chain length of the present polymer nanoparticles were similarly extended, they would have a chain length of 36.5 and 29 nm chain length for P(St-alt-MA)$_{73}$-*b*-PSt$_{81}$ and P(St-alt-MA)$_{58}$-*b*-PSt$_{130}$, respectively, using the same calculation and assuming the same repeat unit length for the St and MA parts of the polymer as for each repeat unit length in PAA. Therefore, the hydrodynamic diameter (D_h) of the nanoparticles should be larger than 73 and 58 nm because double shell chain lengths contribute to D_h. As our DLLS results at pH around 7 and low ionic strength indicate that the particles were much

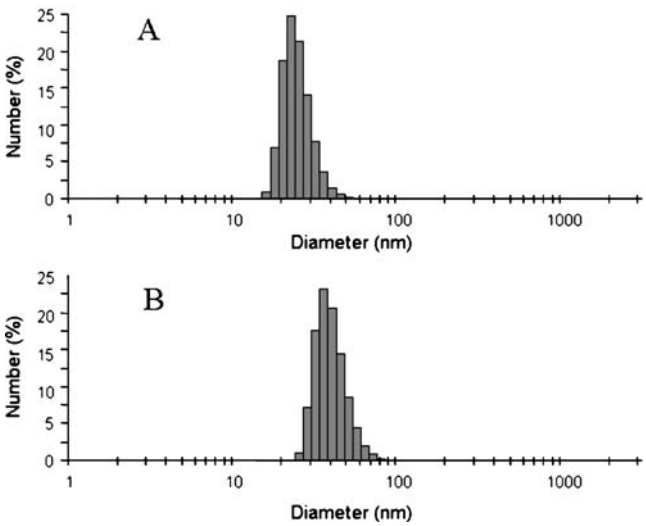

Fig. 5 Particle size distributions, as measured by DLLS, of the diblock copolymer nanoparticles in aqueous suspension. **a** P(St-alt-MA)$_{73}$-*b*-PSt$_{81}$, **b** P(St-alt-MA)$_{58}$-*b*-PSt$_{130}$

smaller than these calculated values, it appears that the outer shell chains of the nanoparticles are not as extended as reported for PAA chains. We postulated that the P(St-alt-MA) chains interact with the hydrophobic PSt core through phenyl groups (Fig. 6) and that these interactions prevent full chain extension under low ionic strength conditions. This hypothesis was supported by TEM (Fig. 2) measurements which indicated that the size of the dried nanoparticles was similar to the size estimated by DLLS, supporting that the outer shell was not able to fully extend in the aqueous system. This result suggested that the shell structure was the major factor influencing the change in particle size between the aqueous and dried state for these nanoparticles.

Measurement of particle size under a range of pH conditions indicated that the particle size varied only a few nanometers over a wide range of pH (Fig. 7). The smallest particle sizes were observed around pH 6. Above pH 8, particle size was constant, suggesting that the P(St-alt-MA) chains stretched to an equilibrium length even when the carboxylic acid groups were not fully ionized. It was postulated that as pH decreased from 8 to 6, the degree of dissociation of carboxylic acid in the outer shell chain decreased, resulting in a stronger interaction with the hydrophobic core and the neighboring chains, thereby causing the P(St-alt-MA) shell to shrink. The increase in particle size seen at pH less than 6 is likely to be due to a change in the association behaviors. The weight-average molar mass and the aggregation number N^{agg} increased to 1.27×10^7 gmol^{-1} and 502 for P(St-alt-MA)$_{58}$-*b*-PSt$_{130}$ and 8.44×10^6 gmol^{-1} and 362 for P(St-alt-MA)$_{73}$-*b*-PSt$_{81}$ at pH 2.5.

Figure 8 shows that the particle size distribution was constant over the polymer particle concentration of 0.025–1.0 mg mL^{-1} at pH 6.95. This may mean that, under these conditions, interactions between the nanoparticles in aqueous media are negligible as suggested by Chio [6].

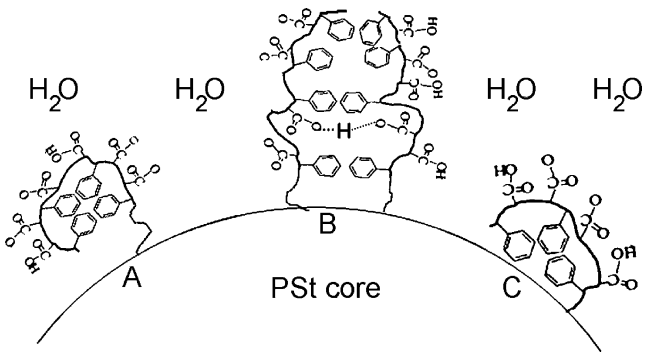

Fig. 6 The postulated structure of P(St-alt-MA)-*b*-PSt nanoparticles in aqueous media. Intrachain interaction (**a**) and interchain interaction (**b**) of the phenyl groups in the P(St-alt-MA) shell chains and the interaction between P(St-alt-MA) chains with the hydrophobic PSt core (**c**)

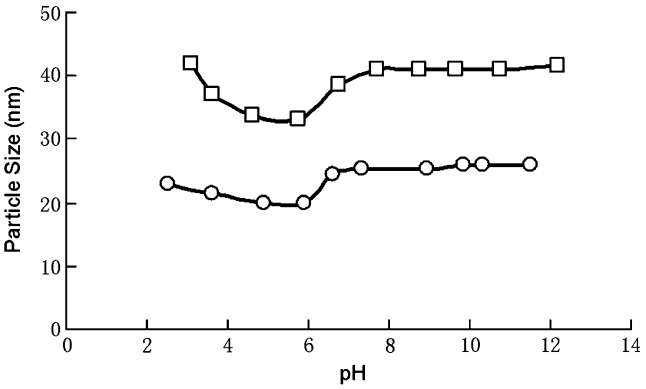

Fig. 7 Particle size of P(St-alt-MA)$_{58}$-*b*-PSt$_{130}$ (*squares*) and P(St-alt-MA)$_{73}$-*b*-PSt$_{81}$ (*circles*) as a function of pH

Although if examined together with the changes observed in the N^{agg} under varying pH values, it may also suggest that some particle–particle aggregation occurs and that the D_h increase is offset by shrinkage due to increased particle–particle electronegative charge interactions. Another interesting finding was that there was negligible change in the hydrodynamic diameter of the particles after 3 months storage at 4 °C (data not shown), which suggests that the self-assembled nanoparticles of P(St-alt-MA)$_m$-*b*-PSt$_n$ were very stable and that particle–particle secondary aggregation did not occur.

The effect of pH on the charge of the self-assembled nanoparticles was determined by measuring their zeta-potential (data not shown). The isoelectric point of the P(St-alt-MA)$_{73}$-*b*-PSt$_{81}$ nanoparticles was approximately pH 2 (0 mV). Above pH 2, the polymer nanoparticles carried a net negative charge with the zeta-potential decreasing to −50 mV at pH 12 due to the dissociation of the carboxylic acid groups. The strong negative charge contributed to the nanoparticle stability due to electrostatic repulsion, creating

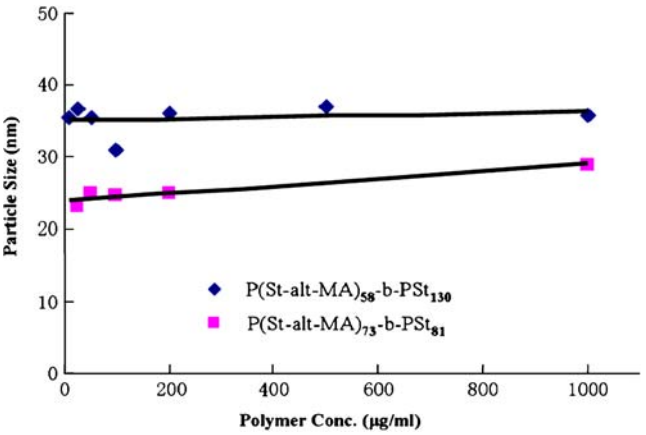

Fig. 8 Particle size of either P(St-alt-MA)$_{58}$-*b*-PSt$_{130}$ or P(St-alt-MA)$_{73}$-*b*-PSt$_{81}$ as function of polymer concentration at pH 6.95

a high electrostatic energy barrier and minimizing particle aggregation [28].

A nanoparticle film, prepared by drying a particle suspension onto a microscope glass slide, was examined by SEM (Fig. 9). The P(St-alt-MA)$_{73}$-*b*-PSt$_{81}$ nanoparticle film surface morphology had a granular structure, indicating its porous nature. An SEM image of a cross-section of a typical dried P(St-alt-MA)$_{73}$-*b*-PSt$_{81}$ nanoparticle film on glass indicated that the nanoparticles were stable both in suspension and in the dried state. No particle–particle coalescence was observed in the dried nanoparticle film. These results suggest that the self-assembled polymeric nanoparticle can be probably used as a new carrier material to prepare dehydrated discrete nanoparticles for use in formulation applications. The nanoparticles had a diameter of approximately 25 nm each supporting the measurements obtained from the DLLS and TEM.

Loading and release of aspirin from the polymer nanoparticles

Aspirin, one of the most frequently used drugs in the treatment of mild to moderate pain, including that of migraines, and fever, has a low solubility in water and is easily decomposed by hydrolysis, making it a relevant model drug to use in loading and release studies. An aspirin loading level of 25% and 19% was obtained for P(St-alt-MA)$_{58}$-*b*-PSt$_{130}$ and P(St-alt-MA)$_{73}$-*b*-PSt$_{81}$, respectively. The difference in the concentration of aspirin able to be entrapped in the two nanoparticles appeared to be due to the length of the hydrophobic polystyrene segments and the aggregation number. The drug loading efficiency was higher in the nanoparticles that had a higher copolymer aggregation number, thereby enabling a greater concentration of drug to be solubilized in their inner core [3, 29]. The

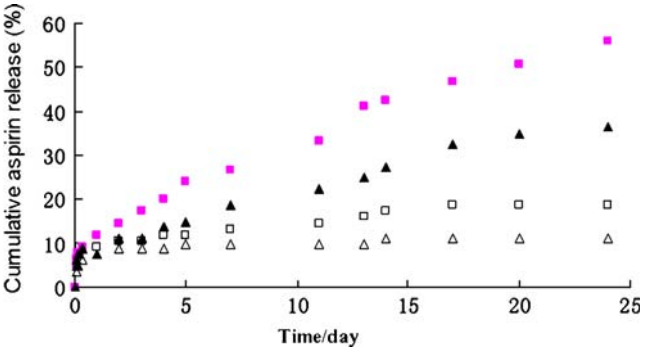

Fig. 10 Cumulative aspirin release profiles from drug-loaded polymer nanoparticles of either P(St-alt-MA)$_{58}$-*b*-PSt130 (*triangles*) or P(St-alt-MA)$_{73}$-*b*-PSt$_{81}$ (*squares*) in distilled water (*unfilled symbol*) or in phosphate buffer solution (pH 7.43, *filled symbol*) at 25 °C

aggregation number of P(St-alt-MA)$_{58}$-*b*-PSt$_{130}$ (N^{agg}, 241) was nearly double than that of the P(St-alt-MA)$_{73}$-*b*-PSt$_{81}$ (N^{agg}, 136). The P(St-alt-MA)$_{58}$-*b*-PSt$_{130}$ copolymer assembled bigger nanoparticles (40 nm) in aqueous media compared to the P(St-alt-MA)$_{73}$-*b*-PSt$_{81}$ (25 nm), which provided more hydrophobic polystyrene core spaces resulting in a higher loading level of aspirin.

The release of aspirin from the nanoparticles was measured as a function of immersion time in two release mediums, water and PBS, at 25 °C (Fig. 10). Approximately 56% and 36% of the aspirin was released from the P(St-alt-MA)$_{73}$-*b*-PSt$_{81}$ and P(St-alt-MA)$_{58}$-*b*-PSt$_{130}$ nanoparticles, respectively, after 25 days immersion in PBS at pH 7.43. In contrast, over the same time, approximately 18% and 11% of the aspirin was released from the P(St-alt-MA)$_{73}$-*b*-PSt$_{81}$ and P(St-alt-MA)$_{58}$-*b*-PSt$_{130}$ nanoparticles immersed in water (pH 6.14), respectively. A control experiment of 2.0 mL aspirin solution (1.0 mg mL^{-1}) in dialysis tubing resulted in more than 98% of aspirin being transferred to

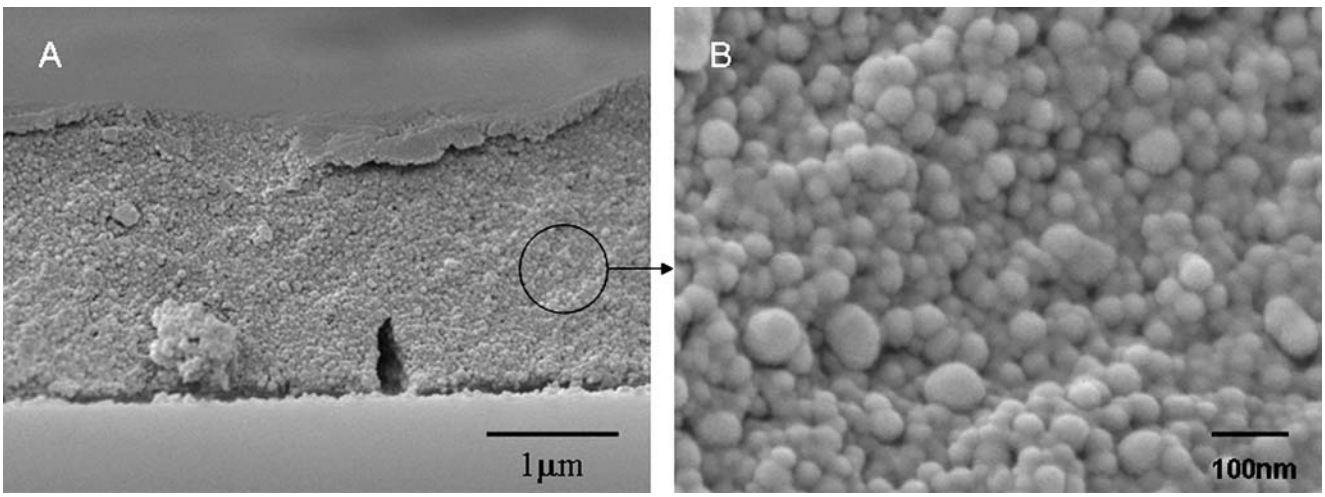

Fig. 9 SEM image of a cross-section of a typical dried P(St-alt-MA)$_{73}$-*b*-PSt$_{81}$ nanoparticle film on glass

the receiving solution within 6 h (data not shown). The lower aspirin release rates observed with the P(St-alt-MA)$_{58}$-*b*-PSt$_{130}$ nanoparticles compared to the P(St-alt-MA)$_{73}$-*b*-PSt$_{81}$ nanoparticles were thought to be due to them having a longer PSt block length and higher N^{agg}. This resulted in them having larger hydrophobic polystyrene cores and particle diameters about 60% larger than the P(St-alt-MA)$_{73}$-*b*-PSt$_{81}$ nanoparticles. Their lower surface area to volume ratio would decrease the diffusion rate of the aspirin [30]. The larger PSt domain may also have slowed water diffusion to the core and led to greater hydrophobic interactions between the PSt blocks and the aspirin, which would both slow the aspirin release rate [30, 31]. Figure 10 also shows that release of aspirin in PBS was faster than in water from both of the two polymer nanoparticles studied, suggesting that both solution conditions (pH and ionic strength) and the properties of the nanoparticles influence the rate at which aspirin is released. The relative contribution of these factors in controlling release is currently being assessed.

Conclusions

A block copolymer based on maleic anhydride and styrene was synthesized via RAFT copolymerization. The hydrolyzed amphiphilic block copolymer formed novel micelle-like nanoparticles by self-assembly in aqueous media. Strong hydrophobic interactions between the PSt segments facilitated aggregate formation. The P(St-alt-MA) outer shell chains interacted with the hydrophobic PSt core through their phenyl groups which prevented the chains from fully extending under aqueous conditions. Particle size remained relatively constant over a range of polymer concentration, and secondary aggregation did not occur over several months storage in low ionic strength media. Particle size and CAC values were dependent upon the composition of the blocked polymer. When the MAn/St molar ratio was increased, the size of the PSt segment of the resulting block polymer decreased, the CAC value of the blocked polymer increased, and the particle size of the nanoparticles decreased. SEM images of a cross-section of the dried nanoparticle film confirmed that particle–particle coalescence did not occur during drying. The release of aspirin from the nanoparticles was dependent on the composition of the block polymer and the release medium.

Acknowledgment This research was funded by the New Zealand Foundation for Research, Science and Technology (Contract CO8X0409, Multiscale Modelling Programme). We thank Liz Girvan and the Otago Centre for Electron Microscopy (OCEM) for the assistance with electron microscopy.

References

1. Kataoka K, Harada A, Nagasaki Y (2001) Adv Drug Deliv Rev 47:113
2. Zhang L, Eisenberg A (1995) Science 268:1728
3. Jones MC, Leroux JC (1999) Eur J Pharm Biopharm 48:101
4. Jeong JH, Kang HS, Yang SR, Kim JD (2003) Polymer 44:583, PII:S0032-3861(02)00816-9
5. Shi L, Zhang W, Yin F, An Y, Wang H, Gao L, He B (2004) New J Chem 28:1038 doi:10.1039/b400445k
6. Choi CY, Chae SY, Kim JD, Jang MK, Cho CS, Nah JW (2005) Bull Korean Chem Soc 26:523
7. Zhang WQ, Shi LQ, An YL, Gao LC, He BL (2004) J Phys Chem B 108:200 doi:10.1021/jp036355x
8. Choi JS, Lee EJ, Park SJ, Kim HJ, Park JS (2001) Bull Korean Chem Soc 22:261
9. Van der Burgh S, Fokkink R, de Keizer A, Stuart MAC (2004) Colloids Surf A 242:167 doi:10.1016/j.colsurfa.2004.04.068
10. Zhu M, Wei L, Zhou P, Du F, Li Z, Li F (2001) Gaofenzi Xuebao 415
11. Zhu M, Wei L, Li F, Jiang L, Du F, Li F, Li F (2001) Chem Commun 365. doi:10.1039/b009815i
12. Feng XS, Pan CY (2002) Macromolecules 35:4888 doi:10.1021/ma020004j
13. Sudalai A, Kanagasabapathy S, Benicewicz BC (2000) Org Lett 2:3213 doi:10.1021/ol006407q
14. Jeong JH, Cho YW, Jung B, Park K, Kim JD (2006) Jpn J Appl Phys Part 1 45:591
15. Pivovarenko VG, Vadzyuk OB, Kosterin SO (2006) J Fluoresc 16:9 doi:10.1007/s10895-005-0020-5
16. Chandar P, Somasundaran P, Turro NJ (1988) Macromolecules 21:950
17. Benoit D, Hawker CJ, Huang EE, Lin Z, Russell TP (2000) Macromolecules 33:1505 doi:10.1021/ma991721p
18. Brouwer HD, Schellekens MAJ, Klumperman B, Monteiro MJ, German A (2000) J Polym Sci A Polym Chem 38:3596
19. Yin XC, Stover HDH (2002) Macromolecules 35:10178 doi:10.1021/ma021110o
20. Yue L, Tao SL, Zhang XH, Wu SH (2005) Gongneng Gaofenzi Xuebao 18:248
21. Zhou N, Lu L, Zhu J, Yang X, Wang X, Zhu X, Zhang Z (2007) Polymer 48:1255 doi:10.1016/j.polymer.2007.01.017
22. Carrillo A, Yanjarappa MJ, Gujraty KV, Kane RS (2005) J Polym Sci A Polym Chem 44:928 doi:10.1002/pola.21219
23. Han SK, Na K, Bae YH (2003) Colloids Surf A 214:49, PII: S0927-7757(02)00389-8
24. Kwon S, Park JH, Chung H, Kwon IC, Jeong SY (2003) Langmuir 19:10188 doi:10.1021/la0350608
25. Wei H, Zhang X, Cheng H, Chen W, Cheng S, Zhuo R (2006) J Control Release 116:266 doi:10.1016j.jconrel.2006.08.018
26. Guo X, Ballauff M (2001) Phys Rev E 64:051406 doi:10.1103/PhysRevE.64.051406
27. Guo X, Ballauff M (2000) Langmuir 23:8719 doi:10.1021/la000319x
28. Kallay N, Zalac S (2002) J Colloid Interface Sci 253:70 doi:10.1006/jcis.2002.8476
29. Hagan SA, Coombes GA, Garnett MC, Dunn SE, Davies MC, Illum L, Davis SS, Harding SE, Purkiss S, Gellert PR (1996) Langmuir 12:2153 doi:10.1021/la950649v
30. Ajun W, Yuxia K (2008) J Nanopart Res 10:437–448 doi:10.1007/s11051-007-9272-0
31. Jeong Y, Na H, Oh J, Choi K, Song C, Lee H (2006) Int J Pharm 322:154 doi:10.1016/j.ijpharm.2006.05.020